Sensitivity and Uncertainty of Reaction Mechanisms for Photochemical Air Pollution

ANDREW H. FALLS, GREGORY J. McRAE, and JOHN H. SEINFELD

Department of Chemical Engineering, California Institute of Technology, Pasadena, California 91125

Abstract

A sensitivity/uncertainty analysis is performed on a mechanism describing the chemistry of the polluted troposphere. General features of the photochemical reaction system are outlined together with an assessment of the uncertainties associated with the formulations of mechanistic details and rate data. The combined effects of sensitivity and uncertainty are determined using the Fourier amplitude sensitivity test (FAST) method. The results of this analysis identify the key parameters influencing the chemistry of NO_2, O_3, and PAN. Based on these findings, a series of recommendations are made for future experimental kinetic studies.

Introduction

A key problem underlying the development and evaluation of kinetic mechanisms for atmospheric chemistry is determining the sensitivity of the concentration predictions to those uncertain aspects of the reaction scheme. Such a determination can serve as a valuable guide for future experimental studies and for identifying those parameters that, when varied within accepted bounds, will be most influential on the predictions of the mechanism.

Although the qualitative aspects of the chemistry of the polluted troposphere appear to be reasonably well understood, there are many important details that still need to be investigated before a complete quantitative understanding of the photochemical smog system is possible. Several groups [1–7] have formulated chemical reaction mechanisms for polluted tropospheric chemistry. Some of these are based on specific surrogate hydrocarbon chemistries [1–4]. In others, attempts have been made to simulate the complex ambient atmospheric system by representing the general features of the hydrocarbon chemistry [2,5–7]. All mechanisms contain aspects of uncertainty, whether in unknown rate constants, in the importance of competing reaction paths, or in the manner of representing

International Journal of Chemical Kinetics, Vol. XI, 1137–1162 (1979)

0538-8066/79/0011-1137$01.00

the reaction of a generalized species. The measure of the accuracy of a mechanism is usually based on the extent of agreement between predicted concentration profiles and those generated experimentally in smog chambers.

Even though the mechanisms [1–7] currently under study differ in details, the basic structure and qualitative behavior of each is similar. Thus, a separate study of the sensitivity of each of the mechanisms is unnecessary.

The object of this work is to examine closely the sensitivity of mechanisms for photochemical smog to those aspects of the chemistry that are currently uncertain. In doing so, it is hoped that certain general features of the photochemical system will emerge; features that are common to all mechanisms and for which estimates of the effect of uncertain parameters will be valuable. A similar study was carried out by Dodge and Hecht [8] in 1975 using the Hecht–Seinfeld–Dodge mechanism [9]. The mechanism of Falls and Seinfeld [7], which includes the latest available information on rate constants, reactions, and has all of the major features present in the lumped mechanisms of Whitten and Hogo [2], Gelinas and Skewes–Cox [5], and Martinez et al. [6] is used in this work. Sensitivity analyses are carried out using the Fourier amplitude sensitivity test (FAST) method of Shuler et al. [10], as described by Koda et al. [11]. Only a brief discussion of the method is given here; extensive details are available in the cited references.

This work begins with a brief discussion of the chemistry of photochemical smog, aimed at elucidating the general structure of the system within which mechanistic and kinetic uncertainties will be evaluated. Next, based on published reports of measured rate constants and product distributions for individual reactions, the uncertainty associated with each element of the Falls and Seinfeld mechanism [7] is estimated. The sensitivity analysis method is then described briefly, with emphasis on the implementation of the parameter uncertainty bounds and interpretation of the results. Finally, the results of the sensitivity analysis are presented and discussed in detail, leading to a ranking of the most influential elements of the mechanism based on the combined effects of uncertainty and sensitivity.

Photochemical Smog Chemistry

NO_2, NO, and O_3 participate in the well-known cyclic set of reactions

$$NO_2 + h\nu \xrightarrow{1} NO + O(^3P)$$

$$O(^3P) + O_2 + M \xrightarrow{2} O_3 + M$$

$$NO + O_3 \xrightarrow{3} NO_2 + O_2$$

In the absence of significant competing reactions, a photostationary state is reached among reactions (1)–(3) in which the steady-state ozone concentration is given by $[O_3]_{ss} = k_1[NO_2]/k_3[NO]$. However, if a process other than that in reaction (3) can convert NO to NO_2 without consuming a molecule of O_3, the ozone concentration will increase due to the increase in the NO_2/NO concentration ratio.

The two main processes by which NO is converted to NO_2, without the loss of ozone, involve the hydroperoxy radical HO_2 and peroxyalkyl radicals RO_2 via

$$HO_2 + NO \rightarrow OH + NO_2$$

$$RO_2 + NO \rightarrow RO + NO_2$$

Hydroperoxy and peroxyalkyl radicals arise in the photochemical smog system from the photolysis and oxidation of hydrocarbon species.

One source of peroxy radicals is from the photolysis of aldehydes that originate in the atmosphere both from emissions and as the products of chemical reactions. Formaldehyde photolysis, at wavelengths less than 370 nm, proceeds by either a molecular or a radical path:

$$HCHO + h\nu \rightarrow H_2 + CO$$

$$\rightarrow H + HCO$$

Both hydrogen atoms and formyl radicals react rapidly with O_2 to produce HO_2 and $HO_2 + CO$, respectively. (There is still some disagreement concerning the $HCO–O_2$ reaction products; however, most evidence indicates that the products are HO_2 and CO.) Higher aldehydes also photodissociate to give alkyl and formyl radicals:

$$RCHO + h\nu \rightarrow R + HCO$$

In addition to their photolysis, the reaction of aldehydes with OH serves as an important radical source and chain carrier. Hydroxyl radicals are generally thought to abstract the aldehydic H atom from aldehydes:

$$OH + RCHO \rightarrow RCO + H_2O$$

Oxidation of hydrocarbon species provides another source of hydroperoxy and peroxyalkyl radicals in the atmospheric system. The key species in the initial oxidation of hydrocarbons is the hydroxyl radical, the major sources of which are indirect chain-related processes such as the photolysis of aldehydes and the reaction of O_3 with olefins which lead to OH radicals through the reaction of HO_2 with NO. Minor sources of the hydroxyl radical include the photolysis of nitrous acid, the photolysis of hydrogen

peroxide, and the reaction of water with singlet oxygen atoms ($O(^1D)$) which originate from the photolysis of ozone:

$$HONO + h\nu \rightarrow OH + NO$$

$$H_2O_2 + h\nu \rightarrow 2OH$$

$$O_3 + h\nu \rightarrow O(^1D) + O_2(^1\Delta_g)$$

$$O(^1D) + H_2O \rightarrow 2OH$$

Hydroxyl radical attack on hydrocarbons leads eventually to a variety of peroxy radicals, such as peroxyalkyl, peroxyacyl, and hydroxy-peroxyalkyl radicals. These radical species convert NO to NO_2, thereby producing ozone, and also serve as sources of alkoxyl, acyl, hydroxy-alkoxyl, and hydroperoxy radicals.

Major Uncertainties in Photochemical Smog Chemistry

With the recent elucidation of the chemistry of the reactions of OH and HO_2 with NO and NO_2 [12,14,15], the inorganic portion of the photochemical smog mechanism is now, by and large, well understood. Table I lists the mechanism under study along with its associated uncertainties. Figure 1 shows the structure and species interaction within the reaction mechanism. Uncertainties to be discussed here include:

(a) Photolysis rates
(b) Alkane–OH product distributions
(c) Olefin–OH and olefin–O_3 product distributions
(d) Aromatic chemistry
(e) Alkoxyl radical reactions
(f) RO_x/NO_x reactions

A major uncertainty in the mechanism lies in the values of the photolysis rate constants. For analyzing smog chamber data, photolysis rate constants relative to the reported value for NO_2 are frequently used. Photolysis rate constants as a function of wavelength can be calculated from

$$k_j = \int_0^\infty \sigma_j(\lambda)\phi_j(\lambda)I(\lambda)\, d\lambda$$

where

k_j = photolysis rate constant for species j
$\sigma_j(\lambda)$ = absorption cross section of species j
$\phi_j(\lambda)$ = quantum yield for the photolysis of species j
$I(\lambda)$ = actinic irradiance

Data applicable to some atmospheric systems have been compiled by Schere and Demerjian [26]. For species such as NO_2, HONO, and O_3, for which extensive experimental determinations of absorption cross sections

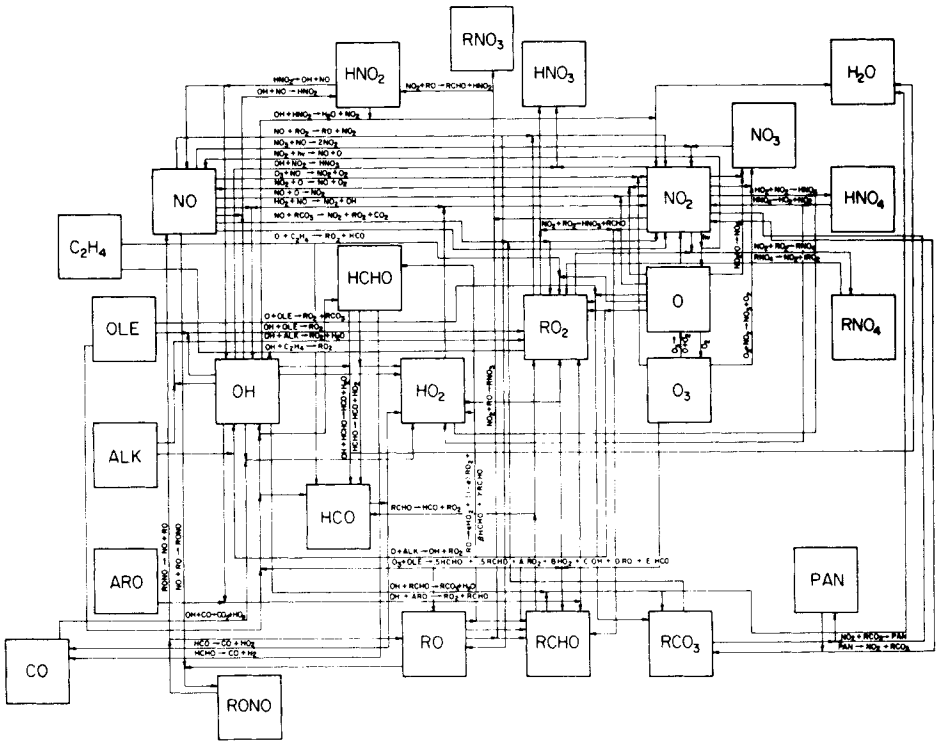

Figure 1. Flow diagram of Falls and Seinfeld reaction mechanism.

and quantum yields have been accomplished, photolysis rate constants are thought to be fairly reliable. However, since cross section and quantum yield data for formaldehyde, higher aldehydes, and alkyl nitrites are much less well characterized, many photolysis rate constants are subjected to large uncertainty. Of course, even if absorption cross sections and quantum yields could be determined accurately for all photosensitive species, uncertainties in atmospheric photolysis rate constants would still exist, as meteorological conditions, clouds, dust, and aerosols cause unknown variances in actinic irradiance.

Whereas rate constants in the inorganic portion of the mechanism are known fairly well, many more uncertainties, both in reaction rate constants and products, are associated with the organic reaction steps. Still to be determined are product distributions and reaction rate constants for the initial steps of the reactions of OH and hydrocarbon species, the largest uncertainties lying in the routes of the various radical species produced. For example, although rate constants for alkane–OH reactions are well established, the ratio of internal to external abstraction for all alkanes is not known. Addition to O_2 to form peroxyalkyl (RO_2) radicals can be

considered as the sole fate of the alkyl radicals first produced in alkane–OH reactions, but after the formation of alkoxyl radicals through the conversion of NO to NO_2, the reaction mechanism becomes uncertain. Alkoxyl radicals can decompose, react with O_2, isomerize, or react with NO or NO_2, with the importance and rate of each reaction path depending on the nature of the alkoxyl group. Even for the most studied of the alkane–OH reactions, the relative rates between decomposition, isomerization, and reaction with O_2, NO, and NO_2 for alkoxyl radicals have not been measured, but must be estimated [3]. The *n*-butane–OH reaction mechanism, for which the ratio of internal to external abstraction is known to be about 86–14 [3], gives rise to *sec*-butoxy and *n*-butoxy radicals. Various possible reaction pathways for these two radicals are:

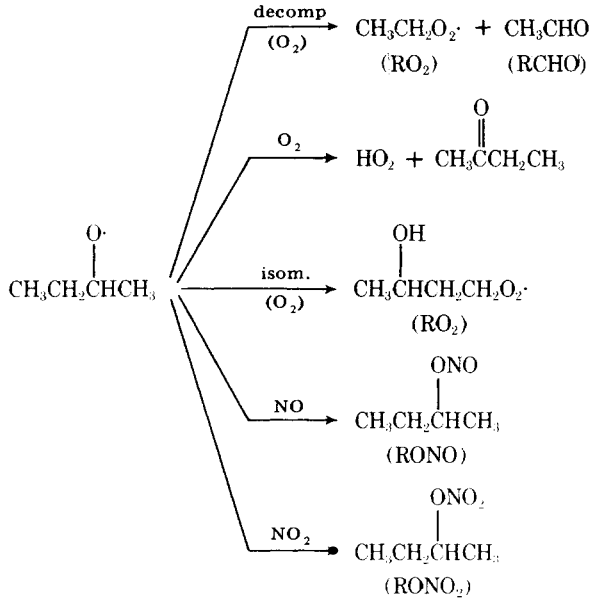

and

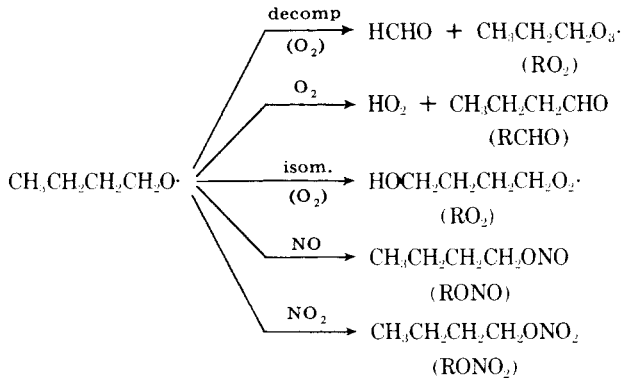

Less well understood than alkane reaction mechanisms are olefin oxidation processes. Whereas reactions of alkanes with O_3 could be neglected, both olefin–OH and olefin–O_3 reactions occur to a significant extent. Olefin–OH reactions may proceed by addition or abstraction [35]. For smaller olefins, the addition path predominates. However, the abstraction fraction increases with the size of the olefin. Along the addition path for terminally bonded olefins, there is uncertainty as to the ratio of internal-to-external addition. Similar to alkyl radicals, the hydroxy-alkyl radicals formed in the initial OH addition to olefins are thought to immediately add O_2 to form hydroxy-peroxyalkyl radicals and thereafter react with NO to give NO_2 and hydroxy-alkoxyl species. The fate of the hydroxy-alkoxyl radicals is subject to speculation, although the analogous alkoxyl reaction paths of decomposition, isomerization, and reaction with NO, NO_2, and O_2 are the most likely possibilities:

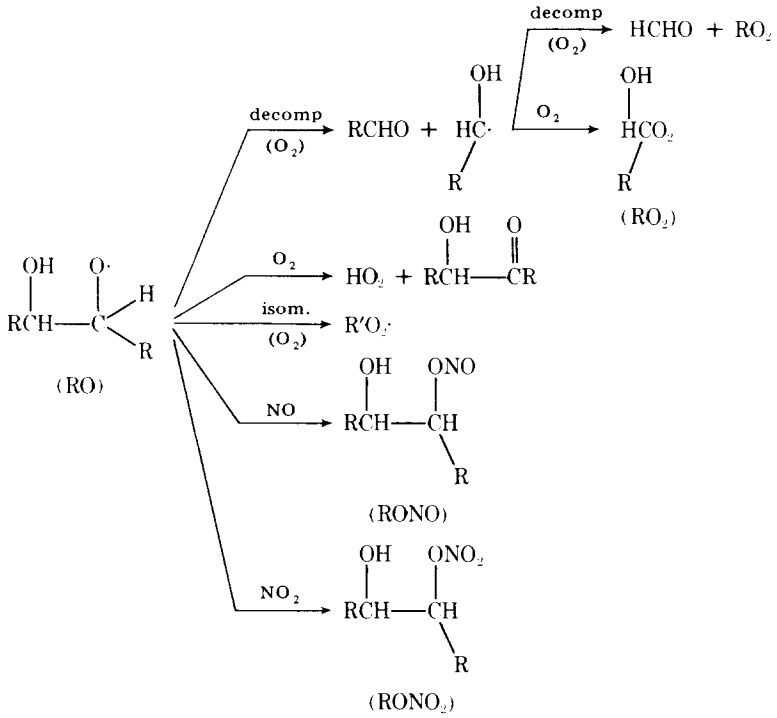

Of some importance in the photochemical smog system is the oxidation of olefins by ozone. The initial rate-determining step in the attack of ozone on the double bond of olefins is the formation of a molozonide, which, as the ring opens, results in a rapid equilibrium between the two possible forms of the oxy-peroxy biradical. The primary uncertainty in the olefin–ozone reaction mechanism lies in the fate of the oxy-peroxy biradical. Currently

it is thought that for lower olefins the biradical decomposes according to the Criegee mechanism of solution phase ozonolosis. However, α- and β-hydrogen abstraction mechanisms have also been proposed [27]. Figure 2 depicts the Criegee mechanism for the gas-phase ozonolosis of a general olefin, with reaction products analogous to those proposed by Dodge [28] for the propylene–O_3 mechanism.

Although much work has been devoted to the understanding of alkane and olefin systems, comparatively little research has been devoted to the study of atmospheric aromatic mechanisms. Recently, absolute rate constants have been determined for the reaction of OH with a series of aromatic hydrocarbons over a range of temperatures [29]. The initial aromatic–OH reaction step can be either abstraction or addition to the ring. At room temperature, the percentage of reaction proceeding by abstraction is on the order of 2–20%, depending on the individual hydrocarbon [29]. The aromatic–OH adduct presumably reacts with other atmospheric species such as O_2, NO, or NO_2. In addition, opening of the aromatic ring presumably occurs at some point in the atmospheric chemistry. Hendry [30] has postulated an aromatic mechanism that accounts for ring cleavage as well as for the formation of oxygenated species such as glyoxal, $H_2C_2O_2$, seen in smog chambers.

The aromatic–OH reaction products in Table I have been represented simply as RO_2 and an oxygenated species that is lumped with the aldehydes. Because the atmospheric chemistry of aromatics is poorly understood, little can be accomplished by speculating on reaction products and mechanisms at this point. For this reason, a sensitivity/uncertainty analysis associated with aromatic species has not been incorporated into this study.

The inherent uncertainty of the decomposition, reaction with O_2, and isomerization of the alkoxyl and hydroxy-alkoxyl radical class in the present mechanism [7] has been concentrated into one reaction step:

$$RO \rightarrow \alpha HO_2 + (1 - \alpha)RO_2 + \beta HCHO + \gamma RCHO$$

As seen from the earlier discussions of alkoxyl radical behavior, RO always gives rise to either HO_2 or RO_2 in any of the decomposition, isomerization, or O_2 reaction pathways. Hence, the stoichiometric coefficients representing the fraction of HO_2 and RO_2 found in the lumped RO reaction should add to 1. Since the RO lumped species represents a large class of different-sized radicals and because splits between reaction paths for even specific radicals are unknown, α can have a value in the range 0 to 1. Many RO reaction routes produce aldehydes with some yielding two, as the one suggested by Martinez et al. [6]. Thus, $0 \leq \beta \leq 1$ and $0 \leq \gamma \leq 1$. Since the composition of the RO radical pool is continually changing during the course of a photooxidation, the actual values of α, β, and γ are functions of time. Thus, the selection of constant values of these coefficients introduces uncertainty.

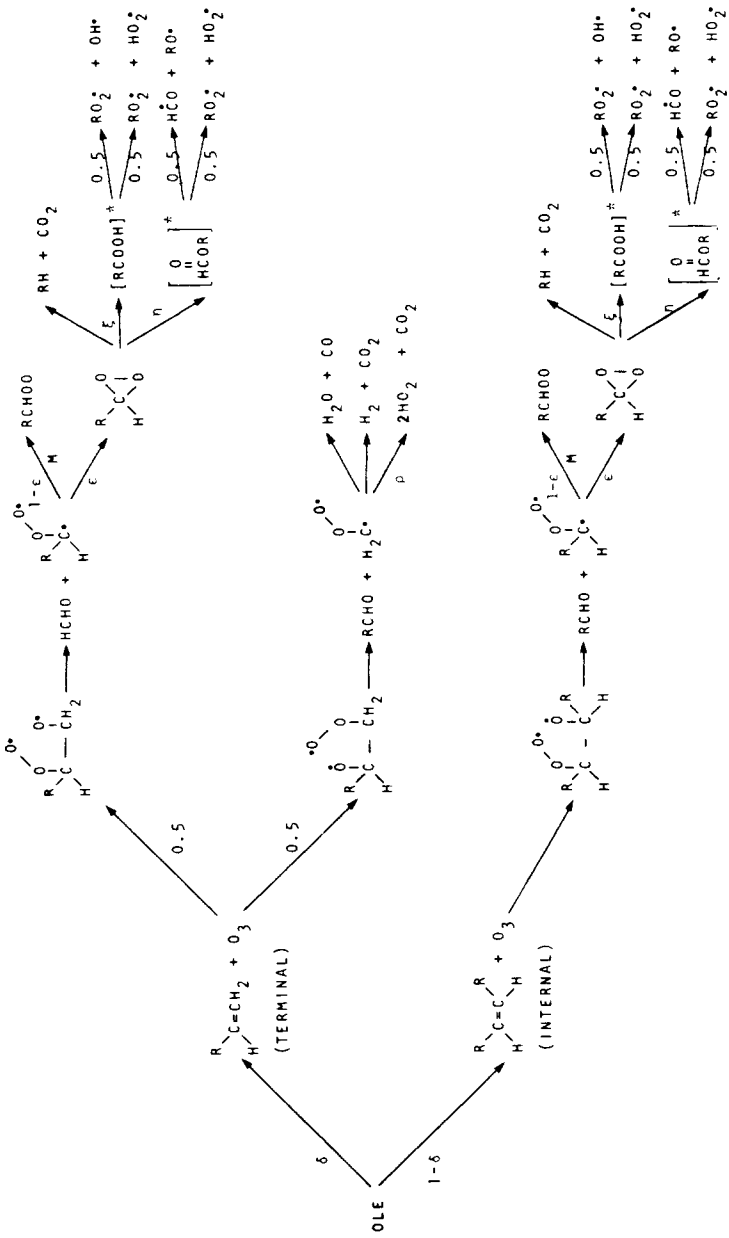

Figure 2. General olefin–ozone reaction mechanism, with reaction products as proposed by Dodge [28].

TABLE I. Uncertainties associated with reaction rate constants in the Falls and Seinfeld mechanism [7].

	Reaction	Nominal rate constant ppm-min units (30°C)	Uncertainty Range[a]	Reference	Sensitivity Uncertainty Analys
1.	$NO_2+h\nu \rightarrow NO+O(^3P)$	variable	$k_1 = \pm 20\%$	(est.)	*
2.	$O(^3P)+O_2+M \rightarrow O_3+M$	2.03×10^{-5}[b]	$1.72\times10^{-5} \leq k_2 \leq 2.38\times10^{-5}$	12	
3.	$O_3+NO \rightarrow NO_2+O_2$	2.55×10^{1}	$1.80\times10^{1} \leq k_3 \leq 3.60\times10^{1}$	12	
4.	$NO_2+O(^3P) \rightarrow NO+O_2$	1.32×10^{4}	$1.15\times10^{4} \leq k_4 \leq 1.52\times10^{4}$	12	
5.	$NO_2+O(^3P) \rightarrow NO_3$	3.52×10^{3}[c]	$2.22\times10^{2} \leq k_5 \leq 5.58\times10^{3}$	12	
6.	$NO+O(^3P) \rightarrow NO_2$	3.87×10^{3}	$2.45\times10^{3} \leq k_6 \leq 6.13\times10^{3}$	12	
7.	$NO_2+O_3 \rightarrow NO_3+O_2$	5.37×10^{-2}	$4.26\times10^{-2} \leq k_7 \leq 6.76\times10^{-2}$	12	
8.	$NO_3+NO \rightarrow 2NO_2$	2.72×10^{4}	$2.12\times10^{4} \leq k_8 \leq 3.31\times10^{4}$	13	
9.	$NO_3+NO_2 \rightarrow N_2O_5$	3.69×10^{3}[c]	$1.06\times10^{3} \leq k_9 \leq 1.21\times10^{4}$	13	
10.	$N_2O_5 \rightarrow NO_3+NO_2$	1.21×10^{1}	-	13	
11.	$N_2O_5+H_2O \rightarrow 2HONO_2$	$<1.45\times10^{-5}$	-	12	
12.	$NO+NO_2+H_2O \rightarrow 2HONO$	2.11×10^{-9}[b]	-	12	
13.	$HONO+HONO \rightarrow NO+NO_2+H_2O$	1.38×10^{-3}	-	12	
14.	$O_3+h\nu \rightarrow O_2+O(^1D)$	variable	$k_{14} = \pm 30\%$	(est.)	
15.	$O_3+h\nu \rightarrow O_2+O(^3P)$	variable	$k_{15} = \pm 30\%$	(est.)	*
16.	$O(^1D)+M \rightarrow O(^3P)+M$	4.14×10^{4}	$3.29\times10^{4} \leq k_{16} \leq 5.21\times10^{4}$	12	
17.	$O(^1D)+H_2O \rightarrow 2OH$	3.34×10^{5}	$2.65\times10^{5} \leq k_{17} \leq 4.21\times10^{5}$	12	
18.	$HO_2+NO_2 \rightarrow HONO+O_2$	$<10^{-3}\ k_{19}$	-	14	
19.	$HO_2+NO_2 \rightarrow HO_2NO_2$	1.58×10^{3}	-	15	
20.	$HO_2NO_2 \rightarrow HO_2+NO_2$	7.5	$3.3 \leq k_{20} \leq 17.1$	15	
21.	$HO_2+NO \rightarrow NO_2+OH$	1.18×10^{4}	$9.59\times10^{3} \leq k_{21} \leq 1.39\times10^{4}$	12	
22.	$OH+NO \rightarrow HONO$	1.74×10^{4}[c]	-	12	
23.	$OH+NO_2 \rightarrow HONO_2$	1.5×10^{4} [c]	$1.31\times10^{4} \leq k_{23} \leq 2.07\times10^{4}$	12	*
24.	$HONO+h\nu \rightarrow OH+NO$	variable	$k_{24} = \pm 30\%$	(est.)	*
25.	$CO+OH \rightarrow CO_2+HO_2$	4.36×10^{2}	$3.46\times10^{2} \leq k_{25} \leq 5.49\times10^{2}$	12	
26.	$OH+HONO \rightarrow H_2O+NO_2$	9.59×10^{3}	$9.15\times10^{2} \leq k_{26} \leq 1.00\times10^{4}$	12	
27.	$HO_2+HO_2 \rightarrow H_2O_2+O_2$	3.63×10^{3}	$1.82\times10^{3} \leq k_{27} \leq 7.26\times10^{3}$	12	
28.	$H_2O_2+h\nu \rightarrow 2OH$	variable	$k_{28} = \pm 30\%$	(est.)	
29.	$OH+O_3 \rightarrow HO_2+O_2$	8.04×10^{1}	$4.03\times10^{1} \leq k_{29} \leq 1.6\times10^{2}$	12	
30.	$HO_2+O_3 \rightarrow OH+2O_2$	3.04	$1.52 \leq k_{30} \leq 6.08$	12	
31.	$HCHO+h\nu \rightarrow 2HO_2+CO$	variable	$k_{31} = \pm 30\%$	(est.)	*
32.	$HCHO+h\nu \rightarrow H_2+CO$	variable	$k_{32} = \pm 30\%$	(est.)	*
33.	$HCHO+OH \rightarrow HO_2+CO$	2.03×10^{4}	$1.62\times10^{4} \leq k_{33} \leq 2.56\times10^{4}$	12	

TABLE I. (*Continued*)

Reaction	Nominal rate constant ppm-min units (30°C)	Uncertainty Range[a]	Reference	Sensitivity/Uncertainty Analysis
34. $RCHO+h\nu \rightarrow RO_2+HO_2+CO$	variable	$k_{34} = \pm 50\%$	(est.)	*
35. $RCHO+OH \rightarrow RCO_3$	2.1×10^4	-	16	
36. $OLE+OH \rightarrow RO_2$	variable[d]	-	17	
37. $OLE+O \rightarrow RO_2+RCO_3$	variable[d]	-	17	
38. $OLE+O_3 \rightarrow 0.5\delta RCHO + (1-0.5\delta)HCHO + [0.5\varepsilon(1-0.5\delta)(\xi+2\eta)+\rho\delta]HO_2 + 0.5\varepsilon(2\xi+\eta)(1-0.5\delta)RO_2 + 0.5\varepsilon\xi(1-0.5\delta)OH + 0.5\varepsilon\eta(1-0.5\delta)RO$	variable[d]	$0 \le \varepsilon \le 1$, $0 \le \xi \le 1$, $0 \le \eta \le 1$ $0 \le \rho \le 1$ Nominal values $\varepsilon = 0.8, \xi = 0.68, \eta = 0.17$ $\delta = 1.0, \rho = 0.1$	17	*
39. $ALK+OH \rightarrow RO_2$	variable[d]	-	17	
40. $ALK+O \rightarrow RO_2+OH$	variable[d]	-	17	
41. $C_2H_4+OH \rightarrow RO_2$	1.14×10^4	$7.06\times10^3 \le k_{41} \le 1.87\times10^4$	12	
42. $C_2H_4+O \rightarrow RO_2+HCO$	1.24×10^3	$1.03\times10^3 \le k_{42} \le 1.49\times10^3$	12	
43. $ARO+OH \rightarrow RO_2+RCHO$	variable[d]	-		
44. $RO \rightarrow \alpha HO_2+(1-\alpha)RO_2 + \beta HCHO+\gamma RCHO$	3.6×10^5	Nominal Values $0 \le \alpha \le 1$ $\alpha=1$ $0 \le \beta \le 1$ $\beta=1$ $0 \le \gamma \le 1$ $\gamma=0$	3	•
45. $NO+RO \rightarrow RONO$	4.9×10^4	$k_{45} = (3.1\times10^4 - 1.55\times10^5)$	18-20	•
46. $RONO+h\nu \rightarrow RO+NO$	variable	$k_{46} = \pm 30\%$	(est.)	*
47. $NO_2+RO \rightarrow RONO_2$	1.55×10^4	$k_{45}/(k_{47}+k_{48}) = (1.2-2.7)$	21-23	•
48. $NO_2+RO \rightarrow RCHO+HONO$	1.35×10^3	$k_{47}/k_{48} = (0.08-0.23)$	21-23	*
49. $NO_2+RO_2 \rightarrow RO_2NO_2$	5.5×10^3	$k_{49} = (1600-5500)$	(est.)	•
50. $NO_2+RO_2 \rightarrow RCHO+HONO_2$	5.5 (est.)	-		
51. $RO_2NO_2 \rightarrow NO_2+RO_2$	0.5 (est.)	$0.55 \le k_{51} \le 40.0$	37	*
52. $NO+RO_2 \rightarrow NO_2+RO$	1.18×10^4 (est.)	$3000 \le k_{52} \le 12000$	(est.)	*
53. $NO+RCO_3 \rightarrow NO_2+RO_2$	3.77×10^3	$k_{54}/k_{53} = 0.54\pm0.17$	25	
54. $NO_2+RCO_3 \rightarrow PAN$	2.03×10^3		25	
55. $PAN \rightarrow NO_2+RCO_3$	0.055	$0.0039 \le k_{55} \le 0.78$	25	
56. $O_3 \rightarrow$ wall loss	variable[e]			
57. $RO_2+RO_2 \rightarrow 2RO+O_2$	196.0	$50.0 \le k_{57} \le 600.0$	38	*

[a] Uncertainties determined from reliabilities in rate constant measurements given in original references. Where no uncertainty was reported, either an estimate was made or the uncertainty neglected.

[b] Units of rate constant are $ppm^{-2}min^{-1}$.

[c] Pseudo-second-order rate constant for 1 atm air.

[d] Rate constants for the reactions of lumped olefins, alkanes, and aromatics with OH, O, and O_3 were taken to be average mole-weighted ratio, based on initial compositions of each hydrocarbon class. Thus $k_l = \Sigma_i k_i n_i / \Sigma_i n_i$ where k_l is the lumped hydrocarbon rate constant, k_i the individual rate constant for hydrocarbon i, and n_i the number of moles of hydrocarbon i in the initial lumped mix.

[e] Depends on smog chamber experiment, Winer [36].

TABLE II. Reactions in the RO_x–NO_x system.

	NO	NO_2
RO	$RO + NO \rightarrow RONO$[a] $\overset{\leftarrow}{h\nu}$ $\rightarrow RCHO + HNO$	$RO + NO_2 \rightarrow RONO_2$[b] $\rightarrow RCHO + HONO$
RO_2	$RO_2 + NO \rightarrow NO_2 + RO$[c] $\rightarrow RONO_2$	$RO_2 + NO_2 \rightleftarrows RO_2NO_2$[d] $\rightarrow RCHO + HONO_2$
RCO_3	$RCO_3 + NO \overset{O_2}{\rightarrow} NO_2 + RO_2 + CO_2$[e]	$RCO_3 + NO_2 \rightleftarrows PAN$[f]

[a] The primary pathway for the alkoxyl–NO reaction is RO + NO → RONO. Rate constants for this series of reactions have not been measured directly, but have been calculated from measured rates of the reverse reaction and thermodynamic estimates. Batt and co-workers [18] obtained rate constants for several of the above reactions that fall in the range of 3.1–6.2 $\times 10^4$ $ppm^{-1}min^{-1}$. Both Mendenhall and co-workers [19] and Batt and Milne [20] determined the rate constant for *t*-butoxyl + NO, obtaining 1.55×10^5 and 6.2×10^4 $ppm^{-1}min^{-1}$, respectively. Thus the probable uncertainty in an estimated value of a particular RO-NO rate constant is a factor of 2–4. In addition to the path shown above there is an abstraction reaction, the fractional occurrence of which depends on the alkyl group. The abstraction fraction can be estimated based on the data of Batt and co-workers [18].

[b] Two reaction paths for alkoxyl–NO_2 reactions exist, addition and abstraction. For methoxyl + NO_2 the abstraction fraction has been estimated by Weibe and co-workers [21] to be 0.08 and by Barker and co-workers [23] to be 0.23. Rate constants for alkoxyl–NO_2 reactions have been inferred from measured values of the ratio of the rate constants of alkoxyl–NO to akoxyl–NO_2 reactions. Wiebe and co-workers [21] reported that for methoxyl radicals this ratio is 1.2, whereas Baker and Shaw [22] obtained 2.7 for the same ratio. Baker and Shaw [22] determined a ratio of 1.7 for *t*-butoxyl radicals. Absolute rate constants for RO–NO_2 reactions are then obtained on the basis of RO–NO rate constants.

[c] The peroxyalkyl radical–NO reaction may proceed as shown. Conversion to NO to NO_2 occurs primarily by the first reaction. It has been postulated that the second reaction will occur a fraction of the time for longer chain peroxyalkyl radicals [$n > 4$]. Darnall and co-workers [32] estimated the ratio k_2/k_1 to be 0.09 and 0.16 for $n = 4$ and 5, respectively. Aside from the HO_2–NO reaction, rate constant values have not been measured for RO_2–NO reactions. A lower limit for the rate constants for these reactions can be estimated as 3×10^3 $ppm^{-1}min^{-1}$ based on theoretical considerations.

[d] Rate constants for the RO_2–NO_2 reaction and the RO_2NO_2 decomposition must be estimated.

[e] Hendry and Kenley [31] report a value of 4900 $ppm^{-1}min^{-1}$ for $CH_3C(O)O_2$+ NO, whereas Cox and Roffey [25] found 3800 $ppm^{-1}min^{-1}$.

[f] The rate constant for the PAN formation step is determined by Hendry and Kenley [31] to be 1500 $ppm^{-1}min^{-1}$ and by Cox and Roffey [25] to be 2070 $ppm^{-1}min^{-1}$. PAN thermal decomposition rates are also reported by the two investigators.

Reactions in the RO_x/NO_x subsystem (Table II) are subject to degrees of uncertainty for two reasons. First, the rate constants reported for spe-

cific reactions in each lumped group differ among investigators. For instance, different PAN formation and decomposition rates have been determined by Cox and Roffey [25] and Hendry and Kenley [31]. Second, since the composition of the lumped radical classes changes throughout the degradation process of the different atmospheric hydrocarbon species, it is difficult to select accurate rate constants for reactions of the RO_x/NO_x system. The uncertainties associated with each reaction in the RO_x/NO_x network are summarized in Table II.

Sensitivity/Uncertainty Analysis

A sensitivity/uncertainty analysis can provide two different but related types of information. By individually perturbing parameters a small amount from their nominal values, say ±5%, the absolute sensitivity of the predictions of the mechanism can be ascertained. A sensitivity/uncertainty analysis incorporates the same information and, in addition, takes into account the degree of uncertainty associated with each parameter, thereby generating a combined measure of sensitivity and uncertainty. Both types of analyses are important. For example, a parameter to which the predictions of the mechanism are not especially sensitive may have such a large range of uncertainty that, when all possible variations are considered, its influence on the predictions is rather substantial. On the other hand, a very sensitive parameter may have a small range of uncertainty, and therefore its overall influence on the mechanism, considering both sensitivity and uncertainty, may be lower than that of other parameters.

In many problems the uncertainties are such that linearized methods are no longer applicable. The FAST method, which overcomes this restriction, has been developed by Shuler et al. [10]. The particular advantage of this approach is that order of magnitude changes in parameter values can be easily accommodated. Basically the procedure involves a simultaneous variation of all the parameters over their individual ranges of estimated uncertainty. Formally the parameters are ranked in the order of importance by using normalized statistical measures called partial variances. These variances indicate the relative contribution of individual parameters to uncertainties in model predictions. The FAST analysis identifies the contribution of individual parameters to the total variance in each predicted species concentration. To determine the sensitivity of the mechanism, the method can be used with each parameter varied a small amount from its nominal value. Detailed descriptions of the technique are available elsewhere [10,11] and will not be repeated here.

Discussion of Results

Two types of the sensitivity/uncertainty analysis were performed on simulations of three different surrogate hydrocarbon smog chamber experiments carried out at the Statewide Air Pollution Research Center at the University of California, Riverside [33,34]. First, in order to ascertain the absolute sensitivity of the predictions of the mechanism to each of the reaction parameters being studied, runs were made in which all parameters of interest were perturbed from their nominal values by ±5%. In a second set of cases, the parameters were permitted to vary over their entire uncertainty range, thus providing combined sensitivity and uncertainty information. The parameter values for these two cases are shown in columns 2 and 3 of Table I. Many of the reactions have been shown to have relatively little influence on concentration behavior [8]. Thus, only those rate constants of reactions for which an asterisk(*) exists in column 4 of Table I were subject to variation in the studies to be described.

Effects of the parameter variations on predictions of NO_2, O_3, and PAN were monitored. These output variables were chosen because air quality standards exist for NO_2 and O_3, and because NO_2 and O_3 reflect the major features of the chemistry. To explore the effects of varying initial hydrocarbon–NO_x mixtures on the results of the study, smog chamber simulations with a wide range of initial conditions were examined. Tables III–VIII list the parameters and their partial variances, ranked according to their effect on each of the output variables, for each of the analyses performed.

TABLE III. Parameter rankings for case 1,[a] small parameter variations.

Time	60 min.		120 min.		180 min.		240 min.		300 min.	
Rank	Parameter	Partial Variance	Parameter	Partial Variance	Parameter	Partial Variance	Parameter	Partial Variance	Parameter	Partial Variance
OUTPUT VARIABLE: NO_2										
1	α	0.310	k_{23}	0.472	k_{23}	0.583	k_{31}	0.354	α	0.320
2	k_{23}	0.309	α	0.310	k_1	0.310	α	0.233	k_{31}	0.286
3	k_{24}	0.193	k_{31}	0.080	α	0.073	β	0.200	β	0.203
4	k_{31}	0.111	β	0.051	k_{31}	0.026	k_1	0.077	k_{23}	0.074
5	β	0.030	k_1	0.025	k_{34}	0.017	k_{34}	0.056	k_{34}	0.051
OUTPUT VARIABLE: O_3										
1	k_1	0.363	k_{23}	0.317	α	0.328	α	0.340	α	0.345
2	α	0.196	α	0.297	k_{23}	0.305	k_{23}	0.278	k_{23}	0.254
3	k_{23}	0.181	k_{31}	0.130	k_{31}	0.148	k_{31}	0.159	k_{31}	0.163
4	k_{24}	0.120	k_1	0.102	β	0.106	β	0.131	β	0.150
5	k_{31}	0.083	β	0.071	k_1	0.038	k_{34}	0.032	k_{34}	0.035
OUTPUT VARIABLE: PAN										
1	k_{23}	0.391	k_{23}	0.485	k_{23}	0.432	k_{23}	0.386	k_{23}	0.350
2	k_{24}	0.212	α	0.187	α	0.213	α	0.230	α	0.245
3	k_{31}	0.153	k_{31}	0.161	k_{31}	0.171	k_{31}	0.181	k_{31}	0.183
4	α	0.128	β	0.078	β	0.110	β	0.135	β	0.153
5	β	0.035	δ	0.026	δ	0.025	k_{34}	0.019	k_{34}	0.020

[a] Simulation: UCR 119J [32]. Initial conditions: $[NO_2] = 0.041$; $[NO] = 0.301$; [OLE] = 0.039; [ALK] = 0.358; [ARO] = 0.070; [ETH] = 0.043; [HCHO] = 0.038; [RCHO] = 0.023; [HONO] (assumed) = 0.0; $k_1 = 0.32$; simulated NO_2 peak time = 200 min; $[HC/NO_x]_0 = 1.7$

TABLE IV. Parameter rankings for case 2,[a] small parameter variations.

Time	60 min.		120 min.		180 min.		240 min.		300 min.	
Rank	Parameter	Partial Variance	Parameter	Partial Variance	Parameter	Partial Variance	Parameter	Partial Variance	Parameter	Partial Variance
OUTPUT VARIABLE: NO_2										
1	k_{31}	0.264	k_{31}	0.378	k_{31}	0.377	α	0.459	α	0.575
2	k_1	0.191	α	0.194	α	0.321	k_{31}	0.338	k_{31}	0.265
3	δ	0.139	k_1	0.112	β	0.104	β	0.105	β	0.095
4	k_{23}	0.128	β	0.091	k_1	0.054	δ	0.023	k_{34}	0.015
5	ε	0.086	k_{23}	0.066	δ	0.039	k_{23}	0.020	δ	0.013
OUTPUT VARIABLE: O_3										
1	k_1	0.473	k_1	0.584	k_1	0.696	k_1	0.778	k_1	0.839
2	α	0.274	α	0.243	α	0.187	α	0.134	α	0.086
3	k_{23}	0.086	k_{23}	0.072	k_{23}	0.071	k_{23}	0.069	k_{23}	0.068
4	k_{31}	0.056	k_{31}	0.043	β	0.021	β	0.009	k_{52}	0.003
5	β	0.032	β	0.035	k_{31}	0.016	k_{31}	0.003	β	0.002
OUTPUT VARIABLE: PAN										
1	k_{23}	0.270	k_{31}	0.290	k_{23}	0.334	k_{23}	0.380	k_{23}	0.404
2	k_1	0.216	k_{23}	0.284	k_{31}	0.306	k_{31}	0.320	k_{31}	0.344
3	k_{31}	0.186	k_1	0.219	k_1	0.199	k_1	0.145	k_1	0.082
4	δ	0.184	δ	0.112	δ	0.091	δ	0.084	δ	0.082
5	ε	0.062	β	0.043	β	0.043	β	0.046	β	0.018

[a] Simulation: UCR-121J [32]. Initial conditions: $[NO_2] = 0.012$; $[NO] = 0.044$; [OLE] = 0.04; [ALK] = 0.37; [ARO] = 0.066; [ETH] = 0.042; [RCHO] = 0.06; [HCHO] = 0.011; [HONO] (assumed) = 0.0; $k_1 = 0.32$; simulated NO_2 peak time = 30 min; $[HC/NO_x]_0 = 10.5$.

TABLE V. Parameter rankings for case 3,[a] small parameter variations.

Time	60 min.		120 min.		180 min.		240 min.		300 min.	
Rank	Parameter	Partial Variance	Parameter	Partial Variance	Parameter	Partial Variance	Parameter	Partial Variance	Parameter	Partial Variance
OUTPUT VARIABLE: NO_2										
1	α	0.289	α	0.423	α	0.433	α	0.441	α	0.445
2	k_{31}	0.167	β	0.226	β	0.238	β	0.240	β	0.232
3	β	0.164	k_{31}	0.197	k_{31}	0.198	k_{31}	0.198	k_{31}	0.200
4	δ	0.112	k_{23}	0.035	k_{23}	0.051	k_{23}	0.048	k_{23}	0.040
5	ε	0.084	δ	0.031	δ	0.015	ε	0.096	δ	0.009
OUTPUT VARIABLE: O_3										
1	α	0.464	α	0.463	α	0.458	α	0.448	α	0.401
2	k_{23}	0.295	k_{23}	0.210	β	0.190	β	0.189	k_1	0.205
3	β	0.083	β	0.155	k_{23}	0.165	k_{23}	0.136	β	0.149
4	k_{31}	0.042	k_{31}	0.094	k_{31}	0.120	k_{31}	0.120	k_{23}	0.117
5	δ	0.027	k_1	0.025	k_1	0.034	k_1	0.075	k_{31}	0.088
OUTPUT VARIABLE: PAN										
1	k_{23}	0.521	k_{23}	0.348	α	0.287	α	0.297	α	0.284
2	α	0.169	α	0.249	k_{23}	0.263	k_{23}	0.227	k_{31}	0.225
3	δ	0.084	β	0.160	β	0.203	β	0.214	k_{23}	0.224
4	β	0.074	k_{31}	0.148	k_{31}	0.188	k_{31}	0.209	β	0.207
5	k_{31}	0.070	δ	0.042	δ	0.026	δ	0.021	δ	0.021

[a] Simulation: EC-237s [32]. Initial conditions: $[NO_2] = 0.021$; $[NO] = 0.075$; [OLE] = 0.030; [ALK] = 0.298; [ARO] = 0.035; [ETH] = 0.175; [HCHO] = 0.0; [RCHO] = 0.001; [HONO] (assumed) = 0.020; $k_1 = 0.30$; simulated NO_2 peak time = 30 min; $[HC/NO_x]_0 = 5.57$.

TABLE VI. Parameter rankings for case 4,[a] large parameter variations.

Time	60 min.		120 min.		180 min.		240 min.		300 min.	
Rank	Parameter	Partial Variance	Parameter	Partial Variance	Parameter	Partial Variance	Parameter	Partial Variance	Parameter	Partial Variance
OUTPUT VARIABLE: NO_2										
1	α	0.933	α	0.831	α	0.854	α	0.846	α	0.826
2	k_{23}	0.018	β	0.055	β	0.091	β	0.105	β	0.122
3	k_{24}	0.011	k_{51}	0.031	k_{51}	0.018	k_{51}	0.009	k_{32}	0.013
4	β	0.010	k_{23}	0.019	δ	0.008	k_{31}	0.009	k_{31}	0.010
5	k_{31}	0.005	ε	0.010	k_{31}	0.006	k_{32}	0.008	δ	0.007
OUTPUT VARIABLE: O_3										
1	α	0.861	α	0.861	α	0.855	α	0.849	α	0.834
2	β	0.033	β	0.065	β	0.086	β	0.097	β	0.106
3	k_{51}	0.029	k_{51}	0.023	k_{51}	0.015	k_{51}	0.010	k_{32}	0.013
4	δ	0.015	δ	0.011	δ	0.008	k_{23}	0.008	k_{23}	0.009
5	ε	0.009	k_{31}	0.007	k_{23}	0.007	δ	0.006	k_{51}	0.006
OUTPUT VARIABLE: PAN										
1	α	0.643	α	0.624	α	0.634	α	0.633	α	0.618
2	β	0.112	β	0.203	β	0.243	β	0.265	β	0.286
3	δ	0.061	δ	0.048	δ	0.031	k_{31}	0.027	k_{31}	0.027
4	k_{51}	0.031	k_{31}	0.030	k_{31}	0.028	δ	0.023	k_{23}	0.020
5	k_{23}	0.028	k_{23}	0.027	k_{23}	0.022	k_{23}	0.020	δ	0.018

[a] Simulation: UCR 119J [32]. Initial conditions: $[NO_2] = 0.041$; [NO] = 0.301; [OLE] = 0.039; [ALK] = 0.358; [ARO] = 0.070; [ETH] = 0.043; [HCHO] = 0.038; [RCHO] = 0.023; [HONO] (assumed) = 0.0; $k_1 = 0.32$; simulated NO_2 real time = 200 min; $[HC/NO_x]_0 = 1.7$.

TABLE VII. Parameter rankings for case 5,[a] large parameter variations.

Time	60 min.		120 min.		180 min.		240 min.		300 min.	
Rank	Parameter	Partial Variance	Parameter	Partial Variance	Parameter	Partial Variance	Parameter	Partial Variance	Parameter	Partial Variance
OUTPUT VARIABLE: NO_2										
1	α	0.535	α	0.677	α	0.695	α	0.685	α	0.665
2	δ	0.223	β	0.139	β	0.158	β	0.169	β	0.173
3	β	0.085	δ	0.085	δ	0.052	k_{51}	0.037	k_{51}	0.030
4	ε	0.046	k_{31}	0.038	k_{31}	0.036	δ	0.037	k_{31}	0.030
5	ω	0.041	ε	0.015	k_{51}	0.019	k_{31}	0.033	δ	0.028
OUTPUT VARIABLE: O_3										
1	α	0.453	α	0.523	α	0.466	α	0.394	α	0.417
2	k_{51}	0.298	k_{51}	0.219	k_{51}	0.198	k_1	0.256	k_1	0.269
3	k_{52}	0.066	k_1	0.097	k_1	0.169	k_{51}	0.150	k_{52}	0.142
4	k_1	0.064	k_{52}	0.078	k_{52}	0.112	k_{52}	0.149	k_{51}	0.073
5	δ	0.032	β	0.037	β	0.015	k_{23}	0.017	β	0.035
OUTPUT VARIABLE: PAN										
1	α	0.454	α	0.505	α	0.568	α	0.644	α	0.699
2	δ	0.229	δ	0.165	δ	0.123	β	0.116	β	0.111
3	k_{51}	0.144	k_{51}	0.105	β	0.122	δ	0.097	δ	0.084
4	β	0.035	β	0.104	k_{51}	0.083	k_{51}	0.053	k_{31}	0.035
5	ω	0.031	k_{31}	0.040	k_{31}	0.042	k_{31}	0.038	k_{51}	0.027

[a] Simulation: UCR-121J [32]. Initial conditions: $[NO_2] = 0.012$; [NO] = 0.044; [OLE] = 0.04; [ALK] = 0.37; [ARO] = 0.066; [ETH] = 0.042; [HCHO] = 0.06; [RCHO] = 0.011; [HONO] (assumed) = 0.0; $k_1 = 0.32$; simulated NO_2 peak time = 30 min; $[HC/NO_x]_0 = 10.5$.

TABLE VIII. Parameter rankings for case 6,[a] large parameter variations.

Time	60 min.		120 min.		180 min.		240 min.		300 min.	
	Parameter	Partial Variance	Parameter	Partial Variance	Parameter	Partial Variance	Parameter	Partial Variance	Parameter	Partial Variance
OUTPUT VARIABLE: NO_2										
1	α	0.697	α	0.691	α	0.649	α	0.237	α	0.240
2	β	0.161	β	0.207	β	0.267	k_{51}	0.205	k_{51}	0.200
3	ε	0.074	k_{51}	0.047	k_{51}	0.031	k_{23}	0.119	k_{23}	0.120
4	k_{51}	0.041	ε	0.028	k_{31}	0.021	k_{31}	0.109	k_{31}	0.110
5	k_{31}	0.125	k_{31}	0.016	δ	0.020	δ	0.098	δ	0.090
OUTPUT VARIABLE: O_3										
1	α	0.718	α	0.742	α	0.716	α	0.650	α	0.589
2	k_{51}	0.161	β	0.098	β	0.149	β	0.227	β	0.285
3	ε	0.043	k_{51}	0.092	k_{51}	0.061	k_{51}	0.044	k_1	0.040
4	k_{52}	0.035	k_{52}	0.025	k_{52}	0.022	k_1	0.028	k_{51}	0.034
5	δ	0.018	k_1	0.013	k_1	0.016	k_{52}	0.019	k_{52}	0.020
OUTPUT VARIABLE: PAN										
1	k_{51}	0.280	β	0.417	β	0.495	α	0.239	α	0.230
2	ε	0.259	α	0.212	α	0.230	k_{51}	0.204	k_{51}	0.119
3	β	0.224	k_{51}	0.144	k_{51}	0.101	k_{23}	0.121	k_{23}	0.118
4	α	0.107	δ	0.130	δ	0.081	k_{31}	0.105	k_{31}	0.100
5	k_{23}	0.080	k_{23}	0.046	k_{31}	0.051	ε	0.091	ε	0.099

[a] Simulation: EC-237s [32]. Initial conditions: $[NO_2] = 0.021$; [NO] = 0.075; [OLE] = 0.030; [ALK] = 0.298; [ARO] = 0.035; [ETH] = 0.175; [HCHO] = 0.0; [RCHO] = 0.001; [HONO] (assumed) = 0.020; $k_1 = 0.30$; simulated NO_2 peak time = 30 min; $[HC/NO_x]_0 = 5.57$.

NO_2 Behavior

The results of the FAST sensitivity/uncertainty analyses help to point out and affirm observations about the qualitative aspects of the chemical mechanism and also provide some new insight into the essential features of the system. The ranking of those parameters to which the predictions of NO_2 behavior are most sensitive highlights the most important of the many mechanisms by which NO_2 is produced. In all the small parameter variation cases, the parameters dominating NO_2 behavior around the time of the NO_2 peak are the photolysis rate, k_1, and the nitric acid formation step. Before and after the predicted peak time, variations in the rates of those reactions forming peroxy radicals, especially the aldehyde photolysis rates, have the most marked effect. In the simulation with the high hydrocarbon to NO_x ratio (case 2), the production of RO_2 and HO_2 from the ozone–olefin reaction is also important.

As discussed earlier, peroxy radicals act to convert NO to NO_2 by

$$RO_2 + NO \xrightarrow{52} RO + NO_2$$

$$HO_2 + NO \xrightarrow{21} OH + NO_2$$

Hence, the rate constants associated with the above reactions, as well as the quantities of RO_2 and HO_2 available, should have a distinct effect on NO_2 concentration levels. The fact that aldehyde photolysis, alkoxyl radical decomposition, and ozone–olefin reactions all produce peroxy radicals explains the large partial variances associated with these parameters. Relative to competing reactions, small variations in k_{52}, the RO_2-NO rate constant, do not produce a large effect on NO_2 predictions. The reason for this is that the RO_2-NO rate constant is so large that other reactions cannot effectively compete for RO_2.

The differences in chemistry brought about by changes in initial conditions are evident from a close examination of the outcome of the larger parameter variation studies, cases 4–6. When the initial hydrocarbon to NO_x ratio is low (case 4), α, the fraction of times that HO_2 is produced from RO, makes the largest contribution to variations in NO_2 predictions. Where initial HC/NO_x levels were higher (case 5), uncertainties in ozone–olefin product distribution and in the production of aldehydes from alkoxyl radicals also contributed significant variances. In systems where initial HC/NO_x ratios are small, or in which fairly unreactive species comprise the hydrocarbon mix, there are not enough radicals present to convert all the available NO to NO_2. As a result, in smog chamber experiments of these systems NO_2 peaks are broad and occur later in the test. For those initial mixtures which are richer in hydrocarbons, or contain very reactive species, there are a larger number of peroxy radicals for the NO_x in the chamber. As the fraction of time that RO_2 is produced from alkoxyl radical reactions is increased (represented by decreasing α), the number of peroxy radicals in the simulation increases. This occurs as a result of the cyclic effect of producing RO_2 from alkoxyl radical reactions and subsequent reconversion to RO through reaction with NO:

$$\mathrm{RO} \xrightarrow{44} (1-\alpha)\mathrm{RO_2} + \alpha\mathrm{HO_2} + \beta\mathrm{HCHO} + \gamma\mathrm{RCHO}$$

$$\mathrm{RO_2} + \mathrm{NO} \xrightarrow{52} \mathrm{RO} + \mathrm{NO_2}$$

Since simulations with low initial HC/NO_x levels can be thought to be radical deficient, α varied over its entire range of uncertainty has a large influence on NO_x predictions. However, α has much less effect on cases in which the initial HC/NO_x ratio is large than when it is small, as other modes of radical production besides RO reactions occur to a significant extent in the high HC/NO_x situation.

O_3 Behavior

Much of the interest in mechanisms for photochemical smog is focused on understanding the avenues for the production of ozone. The results

of the sensitivity analyses are extremely pertinent to this understanding.

Time-varying plots of the partial variances of the major parameters affecting the production of ozone are given in Figures 3–8. As was the case for NO_2 behavior, the results are substantially different for the various initial conditions. For the higher $[HC]/[NO_x]_0$ simulations of cases 2 and 3, small variations in the NO_2 photolysis rate have the biggest impact on ozone formation. On the other hand, at times in the analysis of the low $[HC]/[NO_x]_0$ run (case 1), ozone concentrations are more influenced by peroxy radical production routes. In the large parameter variation cases α dominates the ranked list for low initial HC/NO_x ratios, whereas the other parameters in the alkoxyl radical reaction and the decomposition of the peroxynitrates are also important for high initial HC/NO_x ratios.

The effects of the parameter variations on ozone behavior can be ex-

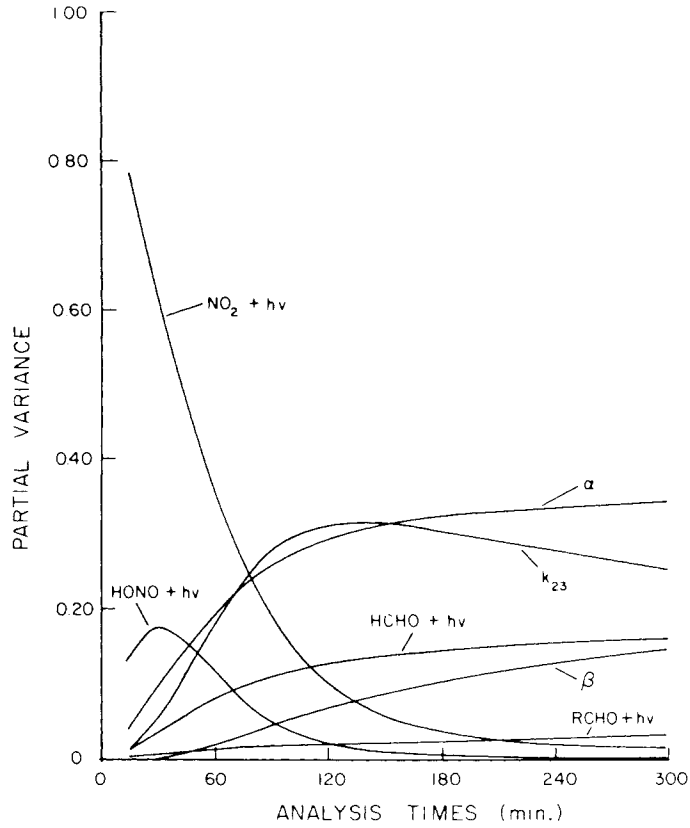

Figure 3. Time-varying partial variances of the major parameters affecting ozone for case 1 (small parameter variation).

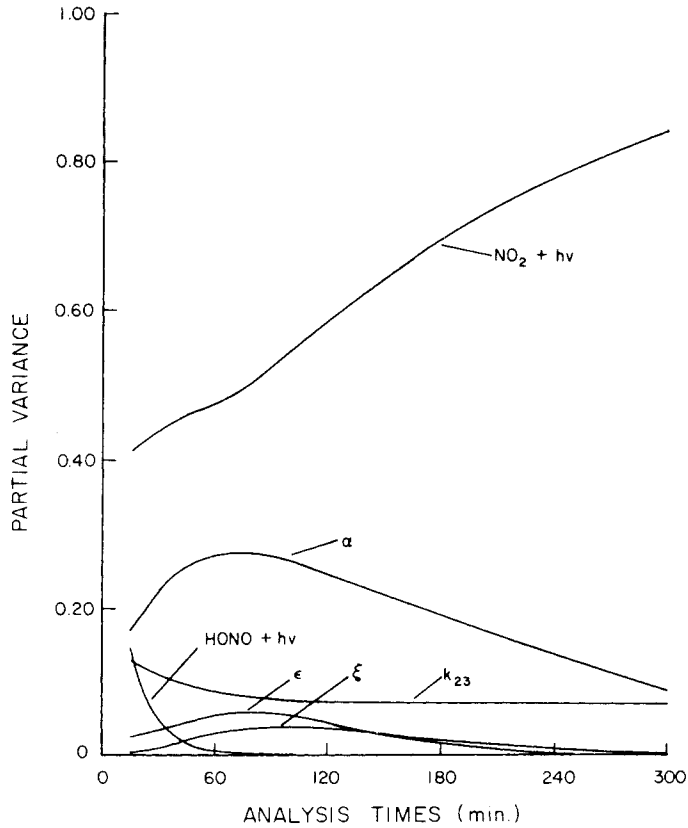

Figure 4. Time-varying partial variances of the major parameters affecting ozone for case 2 (small parameter variation).

plained in much the same fashion as the NO_2 discussion earlier. As can be seen from Figure 1, the ozone level at any time is the result of the complex interplay between NO and NO_2, peroxy radicals, and ozone. Ozone builds up as NO is converted to NO_2 without consuming O_3. When concentration levels of peroxy radicals are low, as in simulations with a lean initial hydrocarbon mix, reactions (1)–(3) exist in a photostationary state. As peroxy radical levels rise, however, the rates of reactions that convert NO to NO_2 without consuming O_3 become comparable to or surpass the rate of reaction (3), modifying the equilibrium set up by reactions (1)–(3). Simulations with low peroxy radical levels will therefore show a much larger sensitivity to those parameters, such as α, which substantially affect the concentrations of the peroxy radicals. When RO_2 levels are higher, as in simulations of high initial HC/NO_x mixtures, there already exists an adequate number of free radicals present to convert NO to NO_2. Hence, the sensitivity of

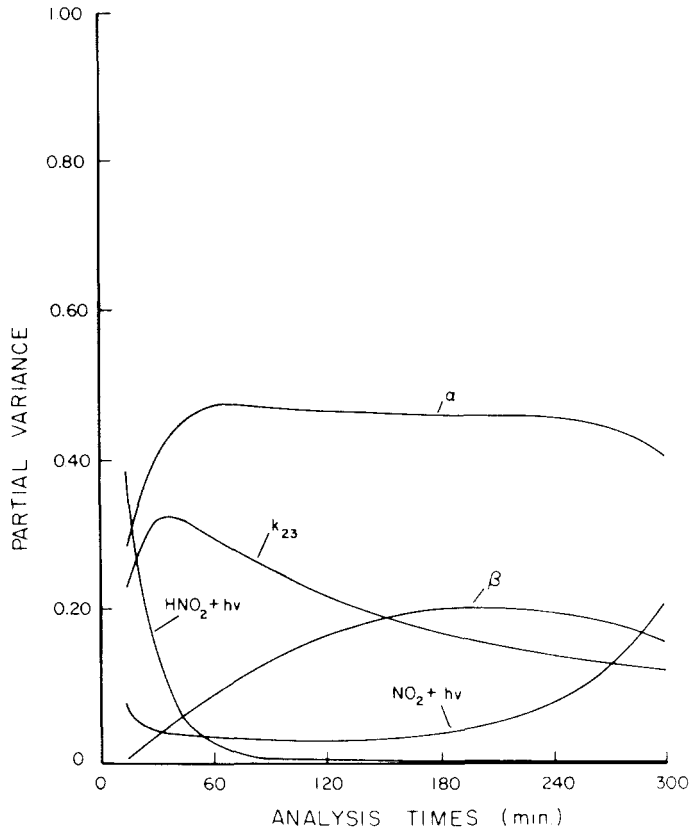

Figure 5. Time-varying partial variances of the major parameters affecting ozone for case 3 (small parameter variation).

the system lies in NO_2 photolysis rates. Moreover, in these systems, the effects of the large variation cases are divided between other parameters which affect the levels of both peroxy radicals and NO_2.

PAN Behavior

PAN predictions are influenced by both NO_2 and RCO_3 concentration levels. Results of the sensitivity/uncertainty analysis can be explained in this light. For case 1, the parameters which highly influence the rate of PAN formation are the nitric acid formation rate constant k_{23} which directly affects the NO_2 level, and the two coefficients α and γ associated with RO decomposition which influences the concentration of RCHO. PAN is affected by RCHO levels because peroxyacyl radicals RCO_3 are formed primarily through the reaction of OH with aldehydes. RCO_3 then

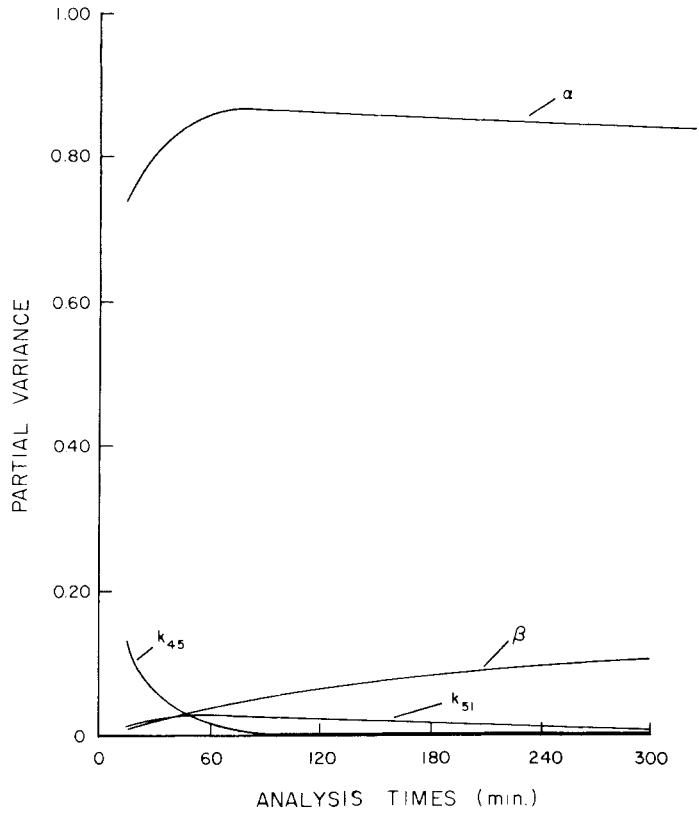

Figure 6. Time-varying partial variances of the major parameters affecting ozone for case 4 (large parameter variation).

reacts with NO_2 to form PAN through a competing reaction with NO. Thus, those parameters that affect RCO_3 production and the availability of OH radicals in the mechanism will subsequently influence PAN levels. For the small parameter variation cases 2 and 3, in which the initial HC/NO_x ratios are higher, parameters perturbing NO_2 levels are much more important in PAN production.

These results are seen even more clearly in the combined sensitivity/uncertainty analyses in cases 4–6. For the low HC/NO_x simulation, the parameters k_{23} and α have large partial variances. The same results are observed in the higher HC/NO_x cases.

Conclusions and Recommendations

Sensitivity and sensitivity/uncertainty analyses have been performed on a representative photochemical smog reaction mechanism. These

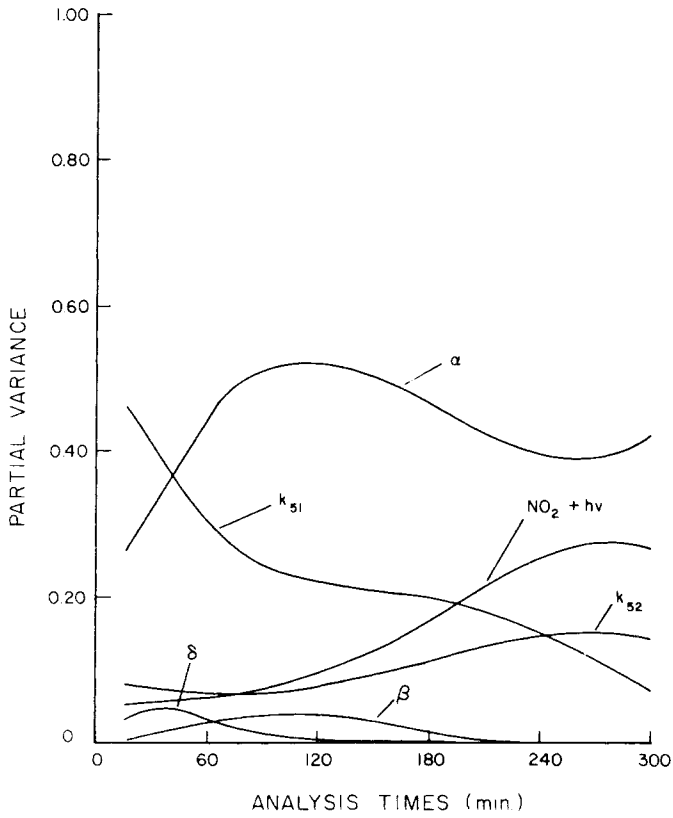

Figure 7. Time-varying partial variances of the major parameters affecting ozone for case 5 (large parameter variation).

studies have shown that the major sensitivity of the NO_2, O_3, and PAN concentrations lies in photolysis rates for NO_2 and aldehydes. On the other hand, when all parameters studied are allowed to vary over their entire ranges of uncertainty, generalized stoichiometric coefficients and certain rate constants have been shown to exert the most influence on the predictions of the mechanism.

Within present experimental uncertainties, the current mechanism for photochemical smog provides a good representation of the chemistry of the major species in the polluted troposphere as evidenced by comparisons of predicted and observed concentrations in smog chamber studies [7]. Based on the sensitivity studies presented here, the level of detail in the treatment of free radical and hydrocarbon chemistry in the mechanism seems to be consistent with the current level of understanding of these processes. However, as additional fundamental studies of alkoxyl radical chemistry, shown by the sensitivity/uncertainty portion of this study to

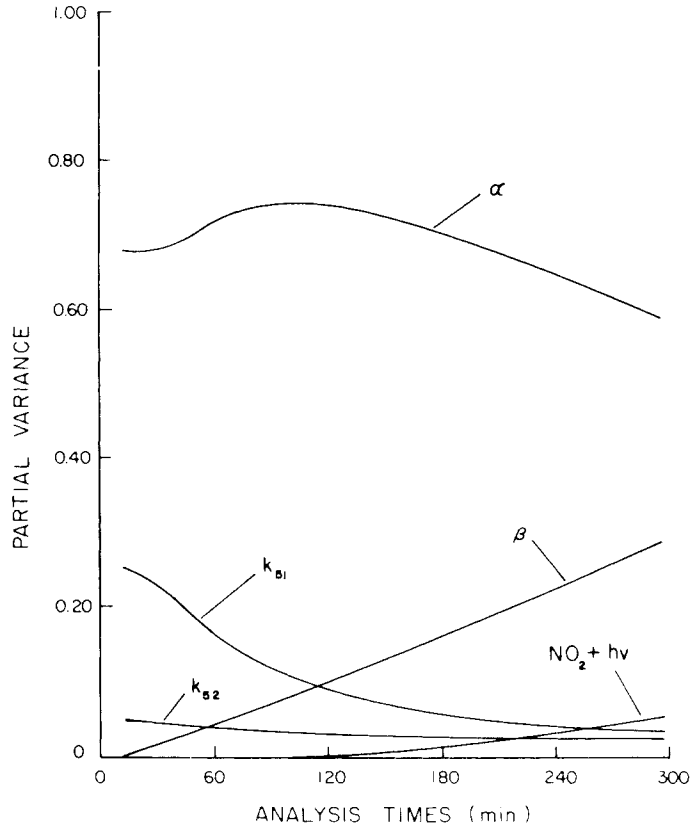

Figure 8.. Time-varying partial variances of the major parameters affecting ozone for case 6 (large parameter variation).

be highly important in the reaction network, are carried out, a more highly resolved radical lumping procedure than is used here may be necessary to improve the accuracy of the mechanism. In addition, when a detailed reaction mechanism for aromatic compounds becomes available, lumped aromatic reaction steps will undoubtedly need to be refined. Because no investigation into the role of aromatics has been attempted in this work, little can be said about the effects such improvements would have on the overall predictions.

In summary, based on these findings, we recommend that experimental work in atmospheric chemistry be concentrated in the following areas:

(a) Studies of decomposition, isomerization, and O_2 reaction pathways of alkoxyl and hydroxyalkoxyl radicals

(b) Improvements in knowledge of the spectral distribution and level

of actinic irradiance for both atmospheric studies and smog chamber experiments

(c) Better measurements of quantum yields and absorption cross sections for aldehydes

and, less importantly, that work be done on:

(d) Olefin–ozone product distributions, needed for accurately modeling systems in which olefins comprise a large fraction of the hydrocarbon mix

(e) Determination of rate parameters associated with the formation and decomposition of peroxynitrates

(f) Determination of emission levels and routine atmospheric measurements of aldehydes, because of their pronounced influence on radical concentrations.

Acknowledgment

This work was supported by the Environmental Protection Agency under grant R805537. Computational resources were provided by the California Air Resources Board under contract A7-187-30. Comments and assistance by Dr. Marcia Dodge and Dr. James Tilden are gratefully appreciated.

Bibliography

[1] T. E. Graedel, L. A. Farrow, and T. A. Weber, *Atmos. Environ.*, **10,** 1095 (1976).

[2] G. Z. Whitten and H. Hogo, "Mathematical Modeling of Simulated Photochemical Smog," Environmental Protection Agency Rep. EPA-600/3-77-011, 1977.

[3] A. C. Baldwin, J. R. Barker, D. M. Golden, and D. G. Hendry, *J. Phys. Chem.*, **81,** 2483 (1977).

[4] W. P. Carter, A. C. Lloyd, J. L. Sprung, and J. N. Pitts, Jr., *Int. J. Chem. Kinet.*, **11,** 45 (1979).

[5] R. J. Gelinas and P. D. Skewes-Cox, *J. Phys. Chem.*, **81,** 2468 (1977).

[6] J. R. Martinez, K. T. Tran, A. C. Lloyd, and G. M. Hidy, "Development of an Atmospheric Model for Sulphate Formation," Environmental Research and Technology, Inc., 1977, Doc. P-1534.

[7] A. H. Falls and J. H. Seinfeld, *Environ. Sci. Technol.*, **12,** 1398 (1978).

[8] M. C. Dodge and T. A. Hecht, *Int. J. Chem. Kinet.*, **1,** 155 (1975).

[9] T. A. Hecht, J. H. Seinfeld, and M. C. Dodge, *Environ. Sci. Technol.*, **8,** 327 (1974).

[10] R. I. Cukier, H. B. Levine, and K. E. Shuler, *J. Comp. Phys.*, **26,** 1 (1978).

[11] M. Koda, G. J. McRae, and J. H. Seinfeld, *Int. J. Chem. Kinet.*, **11,** 427 (1979).

[12] R. J. Hampson, Jr., and D. Garvin, "Reaction Rate and Photochemical Data for Atmospheric Chemistry—1977," NBS Special Rep. Publ. 513, National Bureau of Standards, Washington, DC, 1978.

[13] R. A. Graham and H. S. Johnston, *J. Phys. Chem.*, **82,** 254 (1978).

[14] R. A. Graham, A. M. Winer, and J. N. Pitts, Jr., *Chem. Phys. Lett.*, **51,** 215 (1977).

[15] R. A. Graham, A. M. Winer, and J. N. Pitts, Jr., *J. Chem. Phys.*, **68,** 4505 (1978).

[16] A. C. Lloyd, Workshop on Chemical Kinetic Data Needs for Modeling the Lower Troposphere, Environmental Protection Agency and National Bureau of Standards, Reston, VA, May 15–17, 1978.

[17] G. J. McRae, W. R. Goodin, and J. H. Seinfeld, "Development of a Second Generation Mathematical Model of Photochemical Air Pollution," California Air Resources Board, contract A5-046-87, Final Rep. 1979.
[18] L. Batt, R. D. McCulloch, and R. T. Milne, *Int. J. Chem. Kinet.*, **S1,** 441 (1975).
[19] G. Mendenhall, D. M. Golden, and S. W. Benson, *Int. J. Chem. Kinet.*, **7,** 725 (1975).
[20] L. Batt and R. T. Milne, *Int. J. Chem. Kinet.*, **8,** 59 (1976).
[21] H. A. Wiebe, A. Villa, T. M. Hillman, and J. Heicklen, *J. Am. Chem. Soc.*, **95,** 7 (1975).
[22] G. Baker and R. Shaw, *J. Chem. Soc. (London)*, 6965 (1965).
[23] J. R. Barker, S. W. Benson, and D. M. Golden, *Int. J. Chem. Kinet.*, **9,** 31 (1977).
[24] R. Simonaitis and J. Heicklen, *J. Phys. Chem.*, **78,** 2417 (1974).
[25] R. A. Cox and M. J. Roffey, *Environ. Sci. Technol.*, **11,** 382 (1977).
[26] K. L. Schere and K. L. Demerjian, "Calculation of Selected Photolytic Rate Constants over a Diurnal Range," Environmental Protection Agency Rep. EPA-600/4-77-015, 1977.
[27] H. E. O'Neal and C. Blumstein, *Int. J. Chem. Kinet.*, **5,** 397 (1973).
[28] M. C. Dodge, Workshop on Chemical Kinetic Data Needs for Modeling the Lower Troposphere, Environmental Protection Agency and National Bureau of Standards, Reston, VA, May 15–17, 1978.
[29] R. A. Perry, R. Atkinson, and J. N. Pitts, Jr., *J. Phys. Chem.*, **81,** 296 (1977).
[30] D. G. Hendry, Workshop on Chemical Kinetic Data Needs for Modeling the Lower Troposphere, Environmental Protection Agency and National Bureau of Standards, Reston, VA, May 15–17, 1978.
[31] D. G. Hendry and R. A. Kenley, *J. Am. Chem. Soc.*, **99,** 3198 (1977).
[32] K. R. Darnall, W. P. L. Carter, A. M. Winer, A. C. Lloyd, and J. N. Pitts, Jr., *J. Phys. Chem.*, **80,** 1948 (1976).
[33] J. N. Pitts, Jr., A. M. Winer, K. R. Darnall, G. J. Doyle, and J. M. McAffe, "Chemical Consequences of Air Quality Standards and of Control Implementation Programs: Roles of Hydrocarbons, Oxides of Nitrogen and Aged Smog in the Production of Photochemical Oxidant," California Air Resources Board, contract 4-214, Final Rep., 1976.
[34] A. M. Winer, personal communication, 1978.
[35] J. G. Calvert and R. D. McQuigg, *Int. J. Chem. Kinet.*, **S1,** 113 (1975).
[36] A. M. Winer, personal communication, 1978.
[37] M. C. Dodge, personal communication, 1979.
[38] C. J. Hochanadel, J. A. Ghormley, J. W. Boyle, and P. J. Ogren, *J. Phys. Chem.*, **81,** 3 (1977).

Received September 12, 1978
Revised May 25, 1979
Accepted June 5, 1979